ACS APPLIED MATERIALS & INTERFACES

Research Article

www.acsami.org

Synthesis and Self-Assembly of Large-Area Cu Nanosheets and Their Application as an Aqueous Conductive Ink on Flexible Electronics

Rui Dang,[†,‡] Lingling Song,[†] Wenjun Dong,[*,†] Chaorong Li,[†] Xiaobo Zhang,[†] Ge Wang,[*,‡] and Xiaobo Chen[§]

[†]Center for Optoelectronics Materials and Devices, Department of Physics, Bio-x Center, Zhejiang Sci-Tech University, Hangzhou 310018, China

[‡]School of Materials Science and Engineering, University of Science and Technology Beijing, Beijing 100083, China

[§]CAST Co-operative Research Centre, Monash University, Clayton, VIC 3800, Australia

Supporting Information

ABSTRACT: Large-area Cu nanosheets are synthesized by a strategy of Cu nanocrystal self-assembly, and then aqueous conductive Cu nanosheet ink is successfully prepared for direct writing on the conductive circuits of flexible electronics. The Cu nanocrystals, as building blocks, self-assemble along the ⟨111⟩ direction and grow into large-area nanosheets approximately 30−100 μm in diameter and a few hundred nanometers in thickness. The laminar stackable patterns of the Cu nanosheet circuits increase the contact area of the Cu nanosheets and improve the stability of the conductor under stress, the result being that the Cu nanosheet circuits display excellent conductive performance during repeated folding and unfolding. Moreover, hetero-structures of Ag nanoparticle-coated Cu nanosheets are created to improve the thermal stability of the nanosheet circuits at high temperatures.

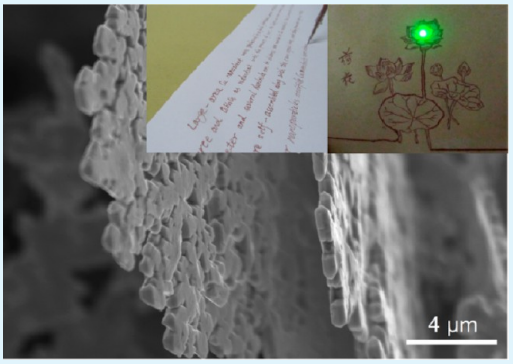

KEYWORDS: *self-assembly, Cu nanosheets, conductive ink, flexible electronics, nanomaterials*

1. INTRODUCTION

In the past decade, flexible electronics, including flexible display,[1−3] flexible antenna arrays,[4,5] flexible radiofrequency identification tags,[6−8] and electronic circuits in clothing,[9,10] have received considerable attention because of their low cost, light weight, and favorable dielectric properties.[11] Until now, many manufacturing techniques such as aerosol-jet printing,[12] inkjet printing, lithography technology,[13] etc., have been developed to fabricate conductive patterns on flexible electronics. However, these technologies involve complicated, time-consuming, and expensive processes.[14] Therefore, researchers are paying more attention to direct writing methods, which can make a desired conductive pattern on various substrates with a one-step procedure.[15] In particular, conductive ink for direct writing on paper substrates remains a priority.

Enormous effort has been devoted to the development of highly conductive ink materials to meet the needs of flexible electronics, such as conductive polymers, organometallic compounds, metal precursors, and nanoscale metallic particles. Conductive polymer circuits exhibit high flexibility, and the manufacturing routes are relatively simple and cost-effective; however, the conductivity is relatively low.[16] Organo-metal or metal precursor-produced circuits represent good conductivity, but additional heat treatment was required to reduce the metallic species.[17] Recently, novel metallic materials such as gold and silver nanostructures have been widely explored in devices as conductive components because of their high conductivity and strong antioxidation properties.[18−20] For example, flexible silver electrocircuits have been fabricated by a silver nanowire inkjet printing method. The printed electrocircuits shows low resistivity in the range from 8.76×10^{-8} to 9.18×10^{-8} Ωm, which fully meet the requirement for application in electrocircuits.[21] Gold/silver nanoparticle-ink printing technology can increase the density of metallic particles, and the conductivity of the pattern can be mediated by the number of the printing layers and the sintering process.[22,23] However, in practical applications, the dispersibility of the nanowire in a viscous solution, the alignment of an individual nanowire in the conductive patterns, and the cracking problem of the nanoparticle-based conductive patterns on flexible and stretch substrate still need to be addressed.[24]

Two-dimensional (2D) nanostructures such as nanodisks and nanosheets exhibit outstanding physical and chemical properties, because of their ability to serve as anisotropic building blocks in terms of their high aspect ratios of the size and thickness.[25] A 2D Cu nanostructure, in particular, is a promising alternative novel metal material for conductive ink because of its low price and high conductivity. To the best of our knowledge, a few strategies have been developed to

Received: October 24, 2013
Accepted: December 6, 2013
Published: December 6, 2013

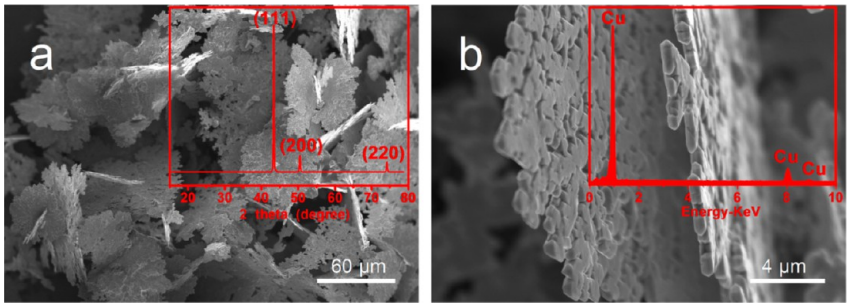

Figure 1. SEM images of Cu nanosheets (a and b) and XRD patterns of Cu nanosheets (inset of panel a) and EDX patterns of Cu nanosheets (inset of panel b).

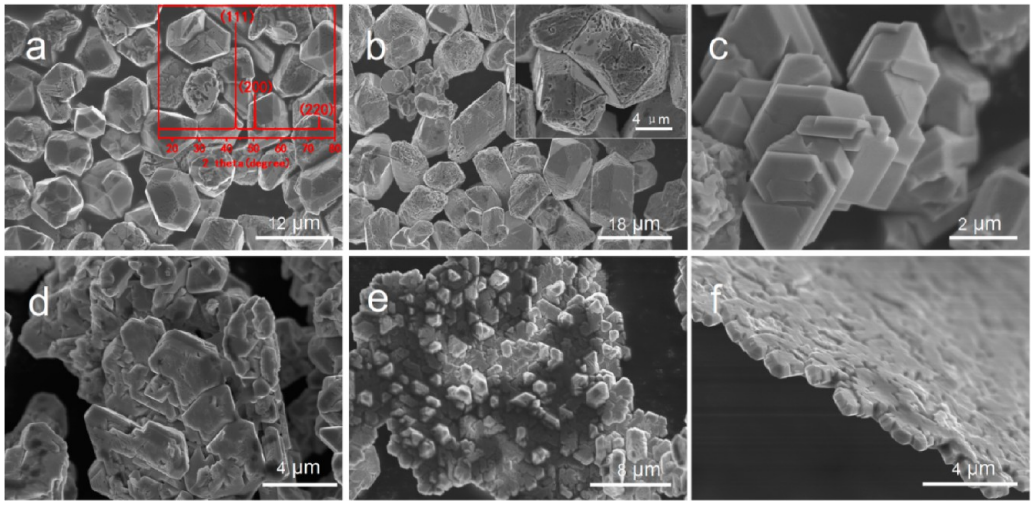

Figure 2. SEM images of as-prepared Cu products at 180 °C for various reaction times: (a) 45, (b) 55, (c) 65, (d) 80, (e) 100, and (f) 180 min. The inset of panel a is the XRD pattern of the sample at 45 min, and the inset of panel b is a high-resolution SEM image.

synthesize 2D Cu nanostructures.[26,27] In particular, large-area Cu nanosheets with high radius/thickness ratios have not been reported. Therefore, an environment-friendly aqueous synthesis strategy capable of generating large-area 2D Cu nanosheets for conductive ink remains a challenge.

Herein, a Cu nanocrystal self-assembly strategy was developed to prepare large-area Cu nanosheets, employing $CuSO_4$ as the Cu source and $C_6H_{12}O_6$ as the reductant in the presence of polyvinyl pyrrolidone (PVP). X-ray diffraction (XRD) and selected-area electron diffraction (SAED) analysis confirmed that Cu nanocrystals, as building blocks, self-assembled along the ⟨111⟩ direction and then grew into large-area Cu nanosheets approximately 30−100 μm in diameter and several hundred nanometers in thickness. Cu nanosheet ink offers a vital opportunity to write alternately stackable Cu nanosheet circuits directly on a flexible substrate. The laminar stackable pattern of Cu nanosheet circuits increases the contact area of the Cu nanosheets and improves the stability of the conductor, the result being that the Cu nanosheet circuits displayed excellent conductive performance during repeated folding and unfolding. Further, hetero-nanostructures of Ag nanoparticle-coated Cu nanosheets were produced by a galvanic displacement reaction, which can improve the thermal stability and conductivity of the Cu nanosheets at high temperatures.

2. EXPERIMENTAL SECTION

Synthesis of Conductive Cu Nanosheets and Ag Nanoparticle-Coated Cu Nanosheets. For the synthesis of Cu nanosheets, 1.0 g of $C_6H_{12}O_6{\cdot}H_2O$, 0.5 g of PVP, and 10 mL of $CuSO_4$ (0.1 mol/L) were dissolved in 25 mL of deionized water while the mixture was being vigorously magnetically stirred, and then the mixture was transferred into a Teflon-lined autoclave and heated at 180 °C for 180 min. The brown-red products were collected, washed three times with deionized water and ethanol, and then dried under vacuum at 60 °C (see Figure S1a of the Supporting Information).

For the synthesis of Ag nanoparticle-coated Cu nanosheets, 3.0 mg of Cu nanosheets was dispersed in 15 mL of deionized water and 0.1 mL of a $AgNO_3$ solution (0.05 mol/L) was added dropwise while the mixture was being vigorously stirred for 5 min. The precipitates were separated from the solution by centrifugation. Then the precipitates were washed three times with deionized water and then dried under vacuum at 60 °C.

Preparation of Cu Nanosheet Ink and Circuits. To prepare Cu nanosheet ink, 4.0 mg of carboxymethyl cellulose (CMC) was dispersed in an aqueous solution containing 12 mL of water and 8 mL of methanol, and the mixture was stirred for 360 min. Cu nanosheets were added to the CMC solution to achieve a desired CMC:Cu weight ratio of 3:100. The mixture was stirred at 4000 rpm for 10 min and allowed to dry in air until a solid loading of 35−65 wt % Cu was obtained (Figure S1b of the Supporting Information). The circuit patterns can be easily drawn with a conductive pen on paper (Figure S1c of the Supporting Information).

Characterization. The morphology and elemental composition of the as-prepared Cu nanosheets were characterized via scanning electron microscopy (SEM) (Hitachi S-4800) and dispersive X-ray spectroscopy (EDX) (Oxford), respectively. Transmission electron

dx.doi.org/10.1021/am404708z | ACS Appl. Mater. Interfaces 2014, 6, 622−629

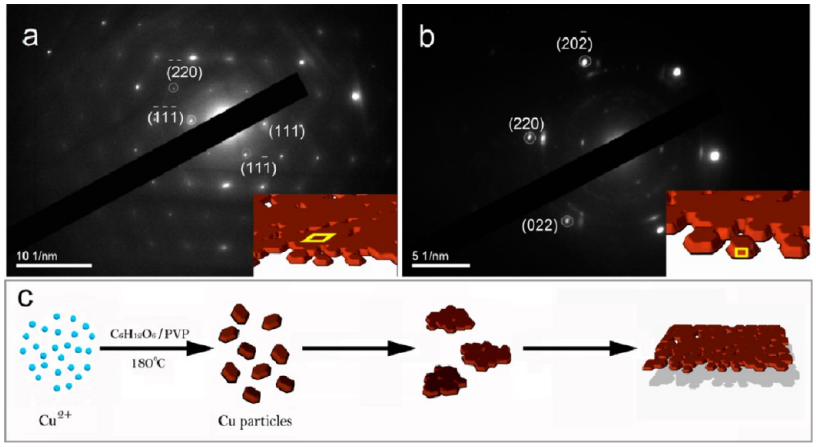

Figure 3. SAED patterns of Cu nanosheets (a and b) and growth mechanism of Cu nanosheets (c).

microscopy (TEM) images and selected-area electron diffraction (SAED) were collected on a JEOL-2010 instrument. XRD patterns were obtained on a Bruker D8-discover instrument operating with Cu Kα radiation (λ = 1.5406 Å). Thermogravimetric analysis (TGA) was conducted in a static air atmosphere (10 °C/min) (shanghai precision scientific instrument ZRY-2P).

3. RESULTS AND DISCUSSION

The morphology of the as-prepared Cu nanosheets reveals its large area 30−100 μm in diameter and several hundred nanometers in thickness (Figure 1a,b). The phase and purity of the as-prepared Cu nanosheets were confirmed by the XRD pattern (inset of Figure 1a). The distinguishable diffraction peaks at 2θ values of 43.3°, 50.4°, and 74.2° correspond to the (111), (200), and (220) crystal planes, respectively, of the face-centered cubic structure (JCPDS No. 04-0836). No impurities were detected, indicating the high purity of products. In addition, the sharp peaks indicated that the product is well-crystallized. EDX analysis further confirmed that the obtained samples were pure Cu nanosheets (inset of Figure 1b).

It is well-known that the intrinsic properties of nanocrystals can be tailored by controlling their size, shape, and structure.[28,29] Understanding the growth mechanism and the shape guiding process of nanocrystals is critical to controlling the shape and size of nanoparticles.[30,31] The evolution of the shape of the Cu nanostructures prepared at 180 °C with different reaction times has been investigated (Figure 2). Figure 2a depicts the SEM image of the sample obtained after 45 min; irregular Cu crystals with 10 μm in diameter on average were produced. XRD diffraction (inset of Figure 2a) reveals its face-centered cubic Cu structure. When the reaction was conducted for 55 min, the Cu nanoparticles, as building blocks, began to aggregate (Figure 2b). The high-resolution SEM image (inset of Figure 2b) shows individual Cu crystals connected with each other, but the outline of the building block was still visible. When the reaction time was increased to 65 min, Cu crystals grew into large blocks (Figure 2c). When the reaction time was extended to 80 min, these Cu nanocrystals self-assembled into sheet structures with a small area approximately 10−20 μm in diameter and 2 μm in thickness (Figure 2d). When the reaction time was increased to 100 min, these small sheets grew into large sheets (Figure 2e). When the reaction time was increased to 180 min, large-area Cu nanosheets approximately 30−100 μm in diameter and 600 nm in thickness with a smooth surface were produced (Figure 2f).

Capping agents have been extensively applied to control the surface energies and growth rates of different facets and therefore the shape assumed by the nanostructures.[32] PVP has been widely used as a surface-capping agent to stabilize the high surface energy in the synthesis of metallic nanoparticles, such as Au, Ag, Pt, and Pd.[33−38] PVP has also had a great impact on the formation of the the resultant Cu products in this study. During the synthesis, carbonyl groups of PVP can coordinate with Cu ions to form complexes, and then the PVP could weaken the catalytic activity of Cu ions on the glucose carbonization reaction.[39−41] The glucose just acted as a reducer in the presence of PVP in the reaction, and then pure Cu products were formed. On the other hand, Cu nanosheets and carbon microspheres were generated simultaneously when the reaction took place in the absence of PVP (see Figure S2a of the Supporting Information), the result being that the carbon mass fraction of the products was increased from 5% (as shown in Figure 1b) to 46% (as shown in Figure S2b of the Supporting Information).

The SAED pattern of Cu nanosheets reveals that the planar surface of the nanosheet was parallel to the {111} facets of the face-centered cubic Cu (Figure 3a), because the electron beam was perpendicular to the sheet. Figure 3b displays a SAED pattern of the lateral surfaces of Cu nanosheets, which is consistent with the {220} plane of Cu. It is well-known that the growth tendency of nanocrystals is determined by the growth rates of different facets.[42] SAED and XRD (insets of panels a and b of Figure 1) analysis confirms that Cu nanosheets grew along the ⟨111⟩ direction. In addition, the thickness of Cu nanosheets was decreased with a prolonged reaction time; small particles on Cu nanosheets gradually disappeared, and eventually, Cu nanosheets with smooth surfaces were produced. The formation of Cu nanosheets is strongly related to the reaction among Cu^{2+}, H_2O, and $C_6H_{12}O_6$, which can be described as follows:

$$CH_2OH(CHOH)_4CHO + H_2O + Cu^{2+} \rightarrow Cu + CH_2OH(CHOH)_4COOH + 2H^+$$

On the basis of the experimental results described above, the growth mechanism of the Cu nanosheet structures is tentatively proposed, and the formation of the Cu nanosheets includes the following three steps (Figure 3c): (1) irregular Cu nanoparticles formed at an early stage, (2) Cu nanoparticles, as building blocks, self-assembled along the ⟨111⟩ direction to

dx.doi.org/10.1021/am404708z | ACS Appl. Mater. Interfaces 2014, 6, 622−629

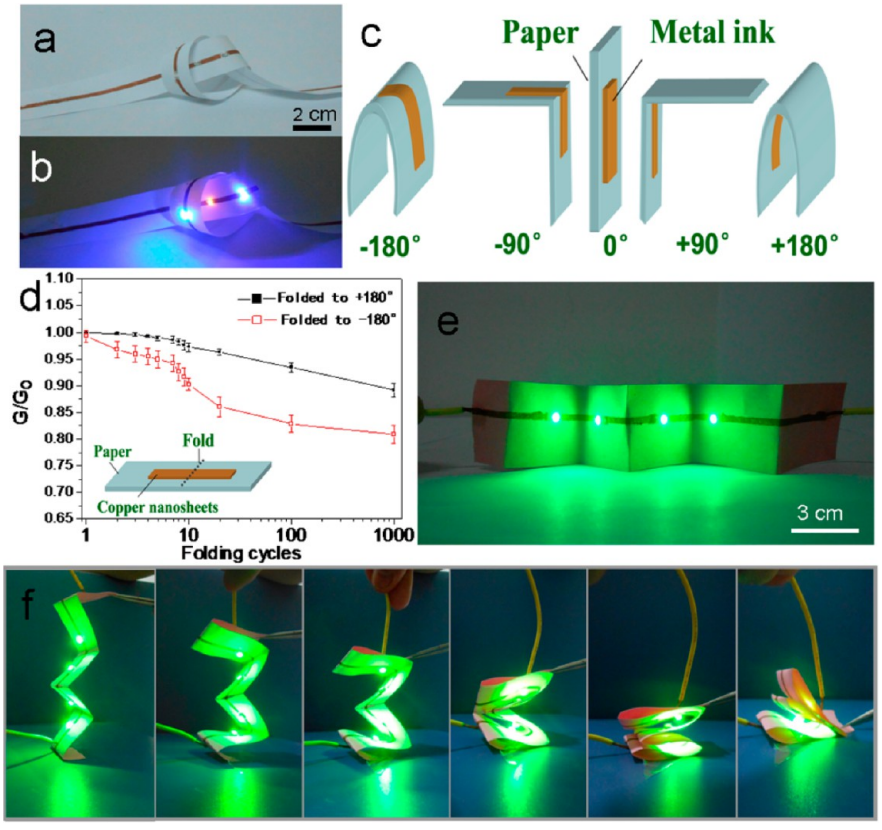

Figure 4. Photographic images of the Cu nanosheet circuit that can support the LED chips on photocopy paper (a) without power and (b) powered by a 9 V battery. (c) Schematic diagrams of various folding angles. (d) Relative conductance of the Cu nanosheet circuits as a function of folding or unfolding cycle. (e) Array of LED chips on a circuit board, including negative and positive angle folding. (f) Bending process of the Cu nanosheet circuits under stress.

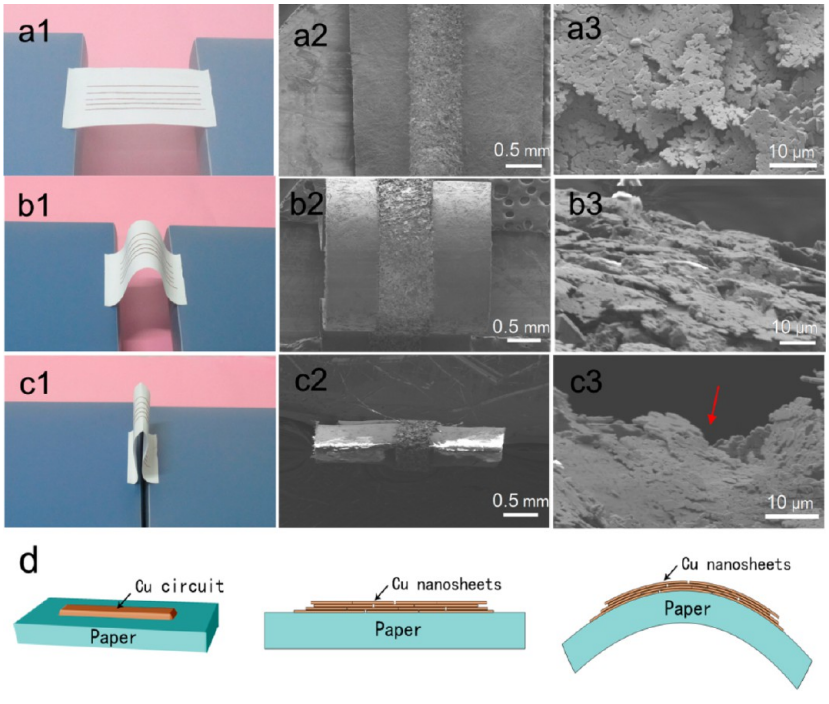

Figure 5. Simulation images (a1−c1), SEM images of folding circuits (a2−c2), and high-resolution images of folding circuits (a3−c3). (d) Schematic diagrams of folding Cu nanosheet circuits.

form small-scale sheets, which is similar to the oriented attachment mechanism,[43] and (3) small-scale sheet structures merged into large-area Cu nanosheets, which is similar to Ostwald ripening.[44]

dx.doi.org/10.1021/am404708z | ACS Appl. Mater. Interfaces 2014, 6, 622−629

Recently, metal ink was found to exhibit very interesting properties as a printing ink on flexible electronics, especially on paper substrates because it is environment friendly, recyclable, foldable, and lightweight.[45−48] Cu nanosheet inks are being considered as a preferable material in flexible electronics, including flexible display, radiofrequency identification, and fabricated electronic circuits, because of the low cost and less electromigration.[49] Cu nanosheet inks can potentially be applied to a variety of functional circuits with complex shapes on paper substrates. For instance, a few LED chips on a Cu nanosheet circuit on photocopy paper were fabricated using a direct writing approach (Figure 4a,b), and the resistivity of the circuit is ∼1.2 × 10^{-7} Ωm. The luminescent strip can maintain its stability after a number of folding and twisting cycles, to cater to various applications. Figure 4c displays various folding angles over the range of −180° to 180°, indicating folding of the Cu nanosheet circuit outside and inside the paper substrate, respectively. As an innovative ink with tremendous potential applications in flexible electronics, it is essential to maintain the conductivity of the mental ink circuits after the folding process. The ratio of the measured conductance (G) to the initial conductance (G_0) of the Cu nanosheet circuits on paper substrates was investigated via repetitive folding and unfolding as demonstrated in Figure 4d. To reduce the deviation, all measurements were repeated five times to obtain an average value. The Cu circuits maintained ∼80.9% of their original conductance after 1000 cycles of −180° folding and ∼89.2% of the onset conductance after 1000 cycles of 180° folding. The Cu nanosheet circuits displayed an excellent stability in terms of conductance on paper substrates. In practical applications, some paper-based electronic circuits need to be folded at either negative or positive angles. A foldable Cu nanosheet circuit board was created by placing LED chips on the paper for negative and positive folding angles (Figure 4e). Figure 4f shows the LED chips performed well on the paper-based circuit board regardless of the folding angle. The Cu nanosheet circuits worked well even when the paper had been fully folded together. The remarkable folding stability indicates not only the good connection between Cu nanosheets but also strong adhesion between Cu nanosheets and paper substrates. Layered conductive structures can slide easily because of the loose interlayer coupling.[50] To investigate the change in the internal structure of the Cu nanosheet circuits after bending, a liner array of five Cu electrodes was produced (width of 750 μm and length of 2 cm) spaced 1.5 mm apart using a conductive pen on photocopy paper and dried at room temperature for 1 h in air. Optical images of the electrode pattern paper substrate in a flat state are shown in Figure 5a1. The corresponding SEM image (Figure 5a2) and the high-resolution images (Figure 5a3) reveal that these Cu nanosheets were spread out and stacked on the paper substrate. When the paper-based circuits were bent slightly (Figure 5b1), the corresponding SEM images show that no trace of cracks or delamination on circuits was observed (Figure 5b2). SEM images demonstrate that these Cu nanosheets overlapped together to form a laminar structure of alternating plates (Figure 5b3 and Figure S3a of the Supporting Information). When the substrate was bent to −180° (Figure 5c1), the SEM image displays a laminar structure of the Cu nanosheets that could bend together with the paper, rather than split on the paper (Figure 5c2,c3 and Figure S3b of the Supporting Information). The laminar structure of nanosheet ciruits can increase the contact area of Cu naosheets under stress and maintain the stability of the conductivity. The schematic diagrams of paper-based circuits of the Cu nanosheet bending process are shown in Figure 5d. In contrast, nanoparticle circuits were prone to forming cracks after bending (Figure S4 of the Supporting Information), because of the weak mutual connection and restriction between nanoparticles.

It is worth noting that the Cu nanosheet ink can be applied to fabricate complicated conductive patterns and devices by a direct writing approach. In addition, the Cu nanosheets and its circuits can work well after being stored under ambient conditions for a long time (see Figures S5 and S6 of the Supporting Information). Cu electrodes, electronic art, and multicolor LED displays on paper substrates were produced by using a conductive pen. The conductive pen consisting of Cu nanosheets can easily be used to write on paper, which further demonstrates strong adhesion between the Cu nanosheet ink and the paper (the optical and SEM images of Cu words are shown in Figure S7 of the Supporting Information). Electronic art, lotus leaves, and Chinese characters were hand-drawn using a conductive pen on photocopy paper. Then a surface-mounted LED chip (3.2 mm × 1.6 mm × 1.1 mm) was set in a gap that was placed in the blossom. After the ink had dried under ambient conditions for 1 h, the LED was illuminated by using a 9 V battery (Figure 6b). Flexible displays have attracted much attention because nanosheets meet the needs of the smaller and higher-density installation design and can be freely bent, folded, and arbitrarily arranged according to spatial layout requirements. To further verify the applicability of the Cu nanosheet ink in large-area flexible displays, an array of multicolor LEDs was fabricated (Figure 6c), in which a series of parallel circuits with 0.6 cm spacing were printed on paper substrate by using a conductive pen. Designed "ZSTU" letters were demonstrated via the placement of LED chips (2.0 mm × 1.2 mm × 1.0 mm). The surface-mounted LED chips were attached to the substrate with silver paste.

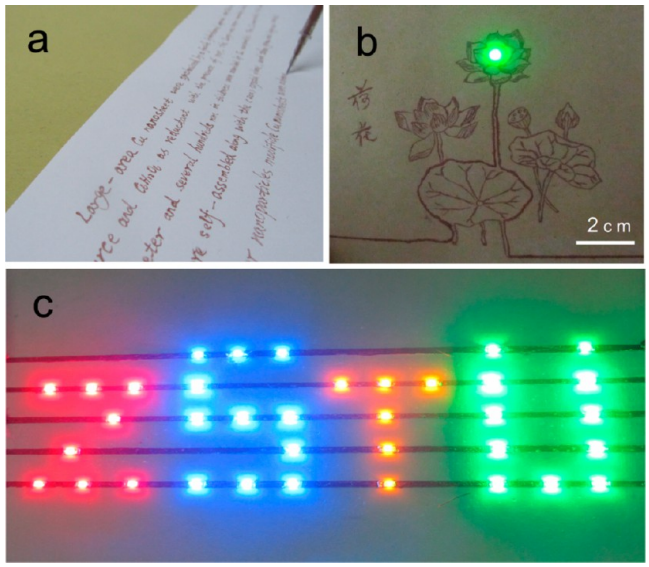

Figure 6. (a) Optical image of a conductive pen loaded with a conductive Cu nanosheet ink. (b) Optical image of drawn conductive electronic art. (c) Optical image of a flexible paper display containing an LED array on paper.

As a kind of conductive material, Cu is widely used in daily life.[51−53] However, Cu can be easily oxidized at high

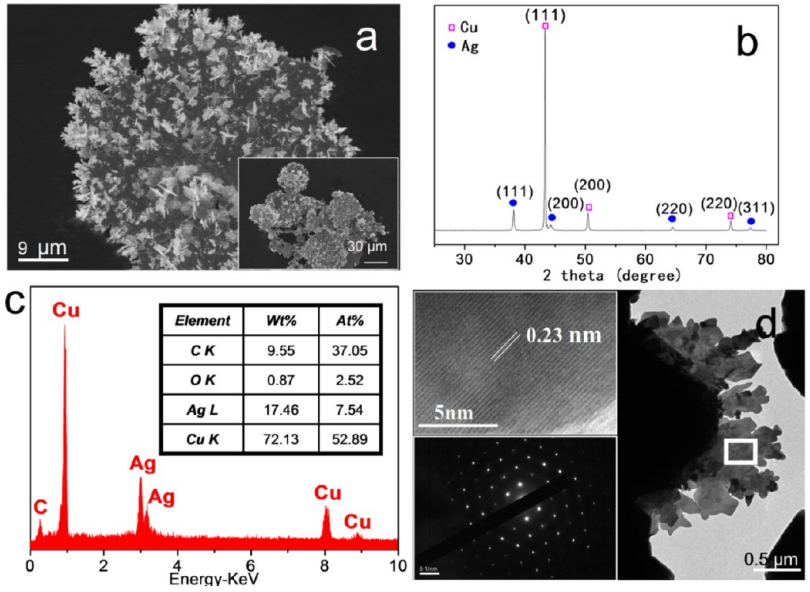

Figure 7. (a) SEM images of Ag nanoparticle-coated Cu nanosheets. (b) XRD patterns of Ag nanoparticle-coated Cu nanosheets. (c) EDX patterns of Ag nanoparticle-coated Cu nanosheets. (d) HRTEM image and SAED pattern of Ag.

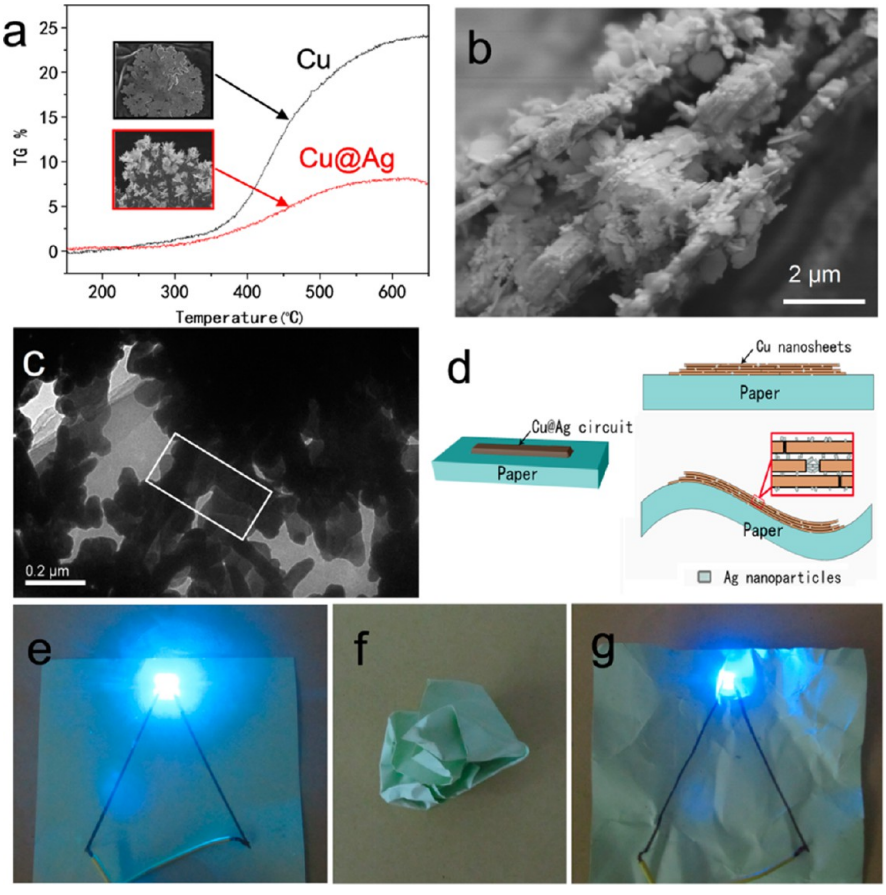

Figure 8. (a) TGA curves of Cu nanosheets and Ag-coated Cu nanosheets. (b) SEM image of a Ag-coated Cu nanosheet circuit. (c) TEM image of Ag-coated Cu nanosheet ink. (d) Schematic diagrams of folding Ag-coated Cu nanosheet circuits (d). (e–g) Operation of a LED chip on the paper-based circuit board before and after it had been crumpled.

temperatures under some specific conditions and with certain requirements. Generally, a Ag coating on Cu was widely applied in the conductive fields because of its excellent conductive property and thermal stability.[54] Herein, Ag nanoparticle-coated Cu nanosheets were prepared by a galvanic displacement method, which can improve the thermal stability of Cu nanosheets at high temperatures. The SEM image (Figure 7a) presents that Ag nanoparticle coating covered the surface of Cu nanosheets. XRD patterns confirmed that the as-prepared Ag nanoparticle is a cubic structure (JCPDS No. 04-0783) (Figure

dx.doi.org/10.1021/am404708z | ACS Appl. Mater. Interfaces 2014, 6, 622–629

7b). EDX analysis reveals that the Ag content of the samples is ~17.5 wt % (Figure 7c). The HRTEM image of Ag reveals a parallel fringe spacing of 0.23 nm, which is consistent with the (111) lattice planes of the cubic Ag, and the corresponding SAED pattern indicates that Ag particles are single-crystal structures (inset of Figure 7d).

The thermoanalytical technique is the most favored technique for the rapid evaluation of the thermal stability of various composites.[55,56] To evaluate the thermal stability of Ag nanoparticle-coated Cu nanosheets, the weight changes of Cu nanosheets and Ag nanoparticle-coated Cu nanosheets were recorded by TGA (shown in Figure 8a). The TGA curves of the two samples had no significant weight gain below 350 °C. The TGA curves of Cu nanosheets displayed an obvious weight gain with an increase in temperature, because of the oxidization of Cu nanosheets. When the temperature reached 650 °C, a weight gain of 24.5% was observed. However, the TGA curve of Ag-coated Cu nanosheets shows a major weight gain of only 7.8% even when the temperature was increased to 650 °C. It confirms that the Ag nanoparticle coating can effectively improve the thermal stability of the Cu nanosheets at high temperatures.

The spatial arrangement of nanoparticles within circuit boards is a crucial factor for the stability of conductance. Ag nanoparticle loading on the surface and edges of Cu nanosheets can effectively improve the area of contact between the layers (shown in Figure 8b). When Ag-coated Cu nanosheets overlap and stack together to form the laminar structure, Ag nanoparticles can act as a conductive intermediary between the Cu nanosheets. In particular, the Ag on the edge of Cu nanosheets can contact another Ag nanoparticle in the same plane attributed to reducing the gap in the adjacent Cu nanosheets (Figure 8c). The bending circuit board of Ag-coated Cu nanosheets shows a laminar structure that is similar to that of the Cu naonosheet circuits; schematic diagrams of Ag-coated Cu nanosheet circuits are shown in Figure 8d. Furthermore, each Ag nanoparticle on the Cu nanosheet can be a good connection point between the interlayer. Ag-coated Cu nanosheet circuit boards with a LED chip were drawn on paper, and the resistivity of the circuit is $\sim 8.9 \times 10^{-8}$ Ωm. The circuit boards worked well after being crumpled and uncrumpled (Figure 8e–g), which demonstrates the Ag-coated Cu nanosheet circuit shows good stability in application. Further research into practical applications, such as the conductance analysis of Ag-coated Cu nanosheet circuits, improvement of the conductive pen, etc., is forthcoming.

4. CONCLUSION

In summary, large-area Cu nanosheets were synthesized by a Cu nanocrystal self-assembly strategy, and aqueous conductive Cu nanosheet ink was successfully prepared by mixing Cu nanosheets in a CMC solution. The large-area Cu nanosheets, assembled by Cu nanocrystal building blocks, were oriented attached along the ⟨111⟩ direction and then self-assembled into large-area nanosheets. The electronic circuits printed by the Cu nanosheet ink revealed an excellent stability of conductance at various folding angles because of the laminar stacked structure of nanosheet circuits. Moreover, a Ag nanocrystal coating on Cu nanosheets effectively improved the thermal stability of Cu nanosheets at high temperatures. The facile and cost-effective method can be a general way to make other kinds of aqueous metal conductive inks on flexible electronics.

■ ASSOCIATED CONTENT

Supporting Information

Production of the conductive pen; synthesis of Ag nanoparticles; optical images of copper nanosheet powder, copper nanosheet ink, and conductive pen; SEM image of samples obtained in the absence of PVP; SEM images of copper nanosheet circuits under different folding angles; SEM image of the Ag-coated particle circuit after being folded; photographic images of the Cu nanosheet circuits prepared for 6 months in air; and SEM image of conductive words. This material is available free of charge via the Internet at http://pubs.acs.org.

■ AUTHOR INFORMATION

Corresponding Authors

*E-mail: wenjundong@zstu.edu.cn.
*E-mail: gewang@mater.ustb.edu.cn.

Notes

The authors declare no competing financial interest.

■ ACKNOWLEDGMENTS

This work was supported by the National Natural Science Foundation of China (51272235 and 21301155), the Zhejiang Provincial Natural Science Foundation of China (LR12E02001 and LY13E020012), the National High-tech R&D Program of China (2013AA031702), the Program for New Century Excellent Talents in University (NCET-13-0998), and the Program for Changjiang Scholars and Innovative Research Team in University (PCSIRT).

■ REFERENCES

(1) Cheon, B. J.; Kim, J. W.; Oh, M. C. *Opt. Express* **2013**, *21*, 4734–4739.
(2) Yoon, B.; Ham, D. Y.; Yarimaga, O.; An, H.; Lee, C. W.; Kim, J. M. *Adv. Mater.* **2011**, *23*, 5492–5497.
(3) Wang, P. C.; MacDiarmid, A. G. *Displays* **2007**, *28*, 101–104.
(4) Anagnostou, D. E.; Gheethan, A. A.; Amert, A. K.; Whites, K. W. *J. Disp. Technol.* **2010**, *6*, 558–564.
(5) Ankireddy, K.; Iskander, M.; Vunnam, S.; Anagnostou, D. E.; Kellar, J.; Cross, W. *J. Appl. Phys.* **2013**, *114*, 124303–124303-5.
(6) Rida, A.; Li, Y.; Vyas, R.; Tentzeris, M. M. *IEEE Trans. Antennas Propag.* **2009**, *51*, 13–23.
(7) Abad, E.; Zampolli, S.; Marco, S.; Scorzoni, A.; Mazzolai, B.; Juarros, A.; Gomez, D.; Elmi, I.; Cardinali, G.; Gomez, J. *Sens. Actuators, B* **2007**, *127*, 2–7.
(8) Li, Y.; Rida, A.; Vyas, R.; Tentzeris, M. M. *IEEE Trans. Microwave Theory Tech.* **2007**, *55*, 2894–2901.
(9) Cherenack, K.; Zysset, C.; Kinkeldei, T.; Münzenrieder, N.; Tröster, G. *Adv. Mater.* **2010**, *22*, 5178–5182.
(10) Bae, J.; Song, M. K.; Park, Y. J.; Kim, J. M.; Liu, M.; Wang, Z. L. *Angew. Chem., Int. Ed.* **2011**, *50*, 1683–1687.
(11) Allen, K. J. *P. IEEE* **2005**, *93*, 1394–1399.
(12) Shankar, R.; Amert, A.; Kellar, J. J.; Whites, K. W. *Nanomater. Energy* **2013**, *2*, 20–24.
(13) Wada, Y. *Microelectron. J.* **1998**, *29*, 601–611.
(14) Lee, H. H.; Chou, K. S.; Huang, K. C. *Nanotechnology* **2005**, *16*, 2436–2441.
(15) Hon, K. K. B.; Li, L.; Hutchings, I. M. *CIRP Annals-Manufacturing Technology* **2008**, *57*, 601–620.
(16) Jang, S. Y.; Marquez, M.; Sotzing, G. A. *J. Am. Chem. Soc.* **2004**, *126*, 9476–9477.
(17) Lee, B.; Jeong, S.; Kim, Y.; Jeong, I.; Woo, K.; Moon, J. *Met. Mater. Int.* **2012**, *18*, 493–498.
(18) Huang, D.; Liao, F.; Molesa, S.; Redinger, D.; Subramanian, V. *J. Electrochem. Soc.* **2003**, *150*, G412–G417.

(19) Lee, K. J.; Jun, B. H.; Kim, T. H.; Joung, J. *Nanotechnology* **2006**, *17*, 2424−2428.
(20) Kim, D.; Moon, J. *Electrochem. Solid-State Lett.* **2005**, *8*, J30−J33.
(21) Zhang, Z.; Zhang, X.; Xin, Z.; Deng, M.; Wen, Y.; Song, Y. *Nanotechnology* **2011**, *22*, 425−601.
(22) Cui, W.; Lu, W.; Zhang, Y.; Lin, G.; Wei, T.; Jiang, L. *Colloids Surf., A* **2010**, *358*, 35−41.
(23) Shankar, R.; Groven, L.; Amert, A.; Whites, K. W.; Kellar, J. J. *J. Mater. Chem.* **2011**, *21*, 10871−10877.
(24) Jang, D.; Kim, D.; Lee, B.; Kim, S.; Kang, M.; Min, D.; Moon, J. *Adv. Funct. Mater.* **2008**, *18*, 2862−2868.
(25) Xu, R.; Xie, T.; Zhao, Y. G.; Li, Y. D. *Cryst. Growth Des.* **2007**, *7*, 1904−1911.
(26) Xu, S.; Sun, X.; Ye, H.; You, T.; Song, X.; Sun, S. *Mater. Chem. Phys.* **2010**, *120*, 1−5.
(27) Zhan, Y. J.; Lu, Y.; Peng, C.; Lou, J. *J. Cryst. Growth* **2011**, *325*, 76−80.
(28) Mayers, B.; Xia, Y. *Chem.—Eur. J.* **2005**, *11*, 454−463.
(29) Chen, X. Z.; Qiu, Z. C.; Zhou, J. P.; Zhu, G. Q.; Bian, X. B.; Liu, P. *Mater. Chem. Phys.* **2011**, *126*, 560−567.
(30) El-Sayed, M. A. *Acc. Chem. Res.* **2001**, *34*, 257−264.
(31) Alivisatos, A. P. *Science* **1996**, *271*, 933−937.
(32) Xia, Y.; Xiong, Y.; Lim, B.; Skrabalak, S. E. *Angew. Chem., Int. Ed.* **2009**, *48*, 60−103.
(33) Li, D. X.; He, Q.; Cui, Y.; Li, J. B. *Chem. Mater.* **2007**, *19*, 412−417.
(34) Tang, X. L.; Jiang, P.; Ge, G. L.; Tsuji, M.; Xie, S. S.; Guo, Y. J. *Langmuir* **2008**, *24*, 1763−1768.
(35) Deivaraj, T. C.; Lala, N. L.; Lee, J. Y. *J. Colloid Interface Sci.* **2005**, *289*, 402−409.
(36) Li, Y.; Boone, E.; El-Sayed, M. A. *Langmuir* **2002**, *18*, 4921−4925.
(37) Wang, H.; Qiao, X.; Chen, J.; Wang, X.; Ding, S. *Mater. Chem. Phys.* **2005**, *94*, 449−453.
(38) Du, Y. K.; Yang, P.; Mou, Z. G.; Hua, N. P.; Jiang, L. *J. Appl. Polym. Sci.* **2006**, *99*, 23−26.
(39) Nishikawa, H.; Tsuchida, E. *J. Phys. Chem.* **1975**, *79*, 2072−2076.
(40) Nishide, H.; Deguchi, J.; Tsuchida, E. *Bull. Chem. Soc. Jpn.* **1976**, *49*, 3498−3501.
(41) Bai, P.; Wu, P. P.; Yan, Z. F.; Zhao, X. S. *Sci. Adv. Mater.* **2011**, *3*, 994−1003.
(42) Wang, Z. L. *J. Phys. Chem. B* **2000**, *104*, 1153−1175.
(43) Cho, K.-S.; Talapin, D. V.; Gaschler, W.; Murray, C. B. *J. Am. Chem. Soc.* **2005**, *127*, 7140−7147.
(44) Morgenstern, K.; Rosenfeld, G.; Comsa, G. *Surf. Sci.* **1999**, *441* (2−3), 289−300.
(45) Manekkathodi, A.; Lu, M. Y.; Wang, C. W.; Chen, L. J. *Adv. Mater.* **2010**, *22*, 4059−4063.
(46) Siegel, A. C.; Phillips, S. T.; Dickey, M. D.; Lu, N.; Suo, Z.; Whitesides, G. M. *Adv. Funct. Mater.* **2010**, *20*, 28−35.
(47) Gao, Y.; Li, H.; Liu, J. *PLoS One* **2012**, *7*, e45485.
(48) Tobjork, D.; Osterbacka, R. *Adv. Mater.* **2011**, *23*, 1935−1961.
(49) Biçer, M.; Şişman, İ. *Powder Technol.* **2010**, *19*, 279−284.
(50) Roth, S.; Baughman, R. H. *Curr. Appl. Phys.* **2002**, *2*, 311−314.
(51) Lu, L.-M.; Zhang, X.-B.; Shen, G.-L.; Yu, R.-Q. *Anal. Chim. Acta* **2012**, *715*, 99−104.
(52) Qin, Y. *J. Catal.* **2004**, *223*, 389−394.
(53) Yang, J.; Chen, J.; Zhou, Y.; Wu, K. *Sens. Actuators, B* **2011**, *153*, 78−82.
(54) Xu, X.; Luo, X.; Zhuang, H.; Li, W.; Zhang, B. *Mater. Lett.* **2003**, *57*, 3987−3991.
(55) Chattopadhyay, D. K.; Webster, D. C. *Prog. Polym. Sci.* **2009**, *34*, 1068−1133.
(56) Freeman, E. S.; Carroll, B. *J. Phys. Chem.* **1958**, *62*, 394−397.